

## Studies of the Energy Dependence of $p$ -O<sup>16</sup> Interactions between 20 and 50 MeV. II. Measurements of the Polarizations of Protons Elastically Scattered by O<sup>16</sup> at 24.5, 27.3, 30.1, 34.1, 36.8, and 39.7 MeV\*

HUDSON B. ELDRIDGE,† S. N. BUNKER, J. M. CAMERON, J. REGINALD RICHARDSON,  
AND W. T. H. VAN OERS‡

*Department of Physics, University of California, Los Angeles, California*

(Received 5 September 1967)

The polarized proton beam from the UCLA sector-focused cyclotron has been used to measure the angular dependence of the polarization in elastic scattering of protons from oxygen at mean proton energies of 24.5, 27.3, 30.1, 34.1, 36.8, and 39.7 MeV. The polarized proton beam was produced by scattering the internal beam from a carbon scatterer. The different proton energies were attained by varying the thickness of the carbon vane and by degrading the external proton beam, using aluminum degraders. A calibration of the beam polarization for the various scatterers was obtained in a separate experiment. A disc of ice 0.032 in. thick by 1.25 in. diam was used as an oxygen target. Four NaI(Tl) integral line detectors were placed two on each side of the incident beam so that protons scattered to the left and to the right at two different angles could be counted at the same time. A solenoid magnet capable of rotating the direction of polarization by  $\pm 180^\circ$  was used, allowing three independent measurements of the left-right asymmetry to be made at each angle. The data obtained for incident proton energies between 30 and 40 MeV exhibit a smooth energy behavior. The data at 24.5 and 27.3 MeV, however, suggest the presence of strong resonances which cause a drastic variation in the polarization angular distribution. A comparison with existing experimental data supports this explanation.

### I. INTRODUCTION

INVESTIGATION of the polarization phenomena in nuclear interactions affords a means of quantitatively determining the extent to which the interaction is spin dependent. Such experimental information subjects existing models of the nuclear interaction, e.g., the nuclear optical model, to a more severe and meaningful test, thereby allowing the investigators to refine the models to correspond more closely to the actual interaction. In the past several years, a number of investigations of the polarization of protons scattered from various nuclei in the medium-energy region,<sup>1-7</sup> i.e., above 20 MeV, have been reported. The analysis of these polarization data combined with the elastic scattering cross sections has been of great importance in the development of the nuclear optical model.

Of the light nuclei, C<sup>12</sup> has received most attention, both experimentally and theoretically. Craig *et al.*<sup>8</sup>

have reported polarizations in the elastic scattering of protons from carbon in the energy region 20–28 MeV. Their results show a nonmonotonic variation with energy in a manner similar to the cross-section data,<sup>9</sup> which is not characteristic of scattering by a complex potential. The analysis by Lowe and Watson<sup>10</sup> showed that the nonmonotonic variation with energy could be explained if a resonant compound elastic contribution from a few states were added to the scattering amplitudes of a complex potential. Going to higher incident proton energies, one should find a smooth variation with energy and thus the optical model should be appropriate in describing the interaction. Available polarization data for proton-carbon elastic scattering above 30 MeV<sup>4-6,8</sup> do not exhibit any marked changes with energy. The existing experimental data on the polarization in the elastic scattering of protons from oxygen<sup>11</sup> show a variation with energy similar to the proton-carbon data. In an analysis of  $p$ -O<sup>16</sup> elastic scattering, Boschitz<sup>12</sup> concluded that the optical model is applicable in the energy region 30–50 MeV, but is less so at lower energies.

In order to study the energy dependence of the optical-model parameters and the resonant effects caused by highly excited states in the compound system F<sup>17</sup>, a self-consistent set of  $p$ -O<sup>16</sup> experimental parameters in the energy region 20–50 MeV has been

\* Supported in part by the U. S. Office of Naval Research, Contract No. 233-(44).

† Present address: Department of Physics, University of Wyoming, Laramie, Wyo.

‡ Present address: Department of Physics, University of Manitoba, Winnipeg, Man., Canada.

<sup>1</sup> R. M. Craig, J. C. Dore, G. W. Greenlees, J. S. Lilley, J. Lowe, and P. C. Rowe, Nucl. Phys. **58**, 515 (1964).

<sup>2</sup> R. M. Craig, J. C. Dore, G. W. Greenlees, J. Lowe, and D. L. Watson, Nucl. Phys. **83**, 493 (1966).

<sup>3</sup> D. L. Watson, J. Lowe, J. C. Dore, R. M. Craig, and D. J. Baugh, Nucl. Phys. **A92**, 193 (1967).

<sup>4</sup> C. F. Hwang, G. Clausnitzer, D. H. Nordby, S. Suwa, and J. H. Williams, Phys. Rev. **131**, 2602 (1963).

<sup>5</sup> L. N. Blumberg, E. E. Gross, A. van der Woude, A. Zucker, and R. H. Bassel, Phys. Rev. **147**, 812 (1966).

<sup>6</sup> M. P. Fricke, E. E. Gross, B. J. Morton, and A. Zucker, Phys. Rev. **156**, 1207 (1967).

<sup>7</sup> R. M. Craig, J. C. Dore, J. Lowe, and D. L. Watson, Nucl. Phys. **86**, 113 (1966).

<sup>8</sup> R. M. Craig, J. C. Dore, G. W. Greenlees, J. Lowe, and D. L. Watson, Nucl. Phys. **79**, 177 (1966).

<sup>9</sup> J. K. Dickens, D. A. Haner, and C. N. Waddell, Phys. Rev. **132**, 2159 (1963).

<sup>10</sup> J. Lowe and D. L. Watson, Phys. Letters **23**, 261 (1966).

<sup>11</sup> E. T. Boschitz, M. Chabre, H. E. Conzett, and R. J. Slobodrian, in *Proceedings of the 2nd International Conference on Polarization Phenomena of Nucleons, Karlsruhe, 1965*, edited by P. Huber and H. Schopper (Birkhauser Verlag, Basel, 1966); E. T. Boschitz (private communication).

<sup>12</sup> E. T. Boschitz, Bull. Am. Phys. Soc. **11**, 355 (1966).

TABLE I. Scatterer and degrader combinations used to obtain the desired beam energies at the target center.

Polarizer thickness (in. of carbon)	Mean energy at polarizer (MeV)	Degrader (gm/cm <sup>2</sup> aluminum)	Mean energy at target center (MeV)	Energy spread of incident beam, full width at half-maximum (MeV)	Polarization of incident beam	Error in polarization (%)
0.019	45.9	0	39.7	1.5	+0.877	±4.0
0.075	44.1	0	36.8	1.8	+0.929	±6.5
0.109	43.0	0	34.1	2.2	+0.896	±4.0
0.109	43.0	0.278	30.1	2.3	+0.896	±4.0
0.109	43.0	0.570	27.3	2.4	+0.896	±4.0
0.109	43.0	0.636	24.5	2.5	+0.896	±4.0

measured. The polarization measurements which are presented in this paper form one of the experimental aspects investigated. Measurements of the elastic differential cross sections have been reported in the preceding paper,<sup>13</sup> and total reaction cross section measurements are currently in progress.<sup>14</sup>

Using a beam of polarized protons produced by scattering the internal beam of the UCLA sector-focused cyclotron from a carbon target, we measured the asymmetries in proton-oxygen elastic scattering at 24.5, 27.3, 30.1, 34.1, 36.8, and 39.7 MeV. The asymmetries were measured over the range of center-of-mass (c.m.) angles 15°–165°. The calibration of the beam polarization was obtained indirectly from asymmetry measurements using a carbon target.

## II. EXPERIMENT

### A. Definitions

If a beam of polarized protons is incident upon a target, there will be an azimuthal asymmetry in the scattered beam. For a beam of spin- $\frac{1}{2}$  particles of polarization  $\mathbf{P}_i$  scattered from a spin-0 target the intensity observed after scattering is

$$I(\theta, \phi) = I_0(\theta) \{1 + \mathbf{P}_i \cdot \mathbf{A}\}.$$

Here  $I_0(\theta)$  is the intensity that would be observed at a scattering angle  $\theta$  if the incident beam were unpolarized. The vector quantity  $\mathbf{A}$  may be expressed as

$$\mathbf{A} = A \hat{n},$$

where

$$\hat{n} = \mathbf{k}_i \times \mathbf{k}_f / |\mathbf{k}_i \times \mathbf{k}_f|,$$

$\mathbf{k}_i$  and  $\mathbf{k}_f$  being the momenta of the incident particle before and after the scattering. In the expression above,  $\phi$  is the angle between  $\mathbf{P}_i$  and  $\mathbf{A}$ . If one takes the direction of  $\mathbf{P}_i$  as pointing vertically downwards, which is the case for the polarized beam from the UCLA cyclotron, one can derive

$$P_i A = \epsilon = \frac{I(\theta, 0) - I(\theta, \pi)}{I(\theta, 0) + I(\theta, \pi)},$$

where  $I(\theta, 0)$  and  $I(\theta, \pi)$  are the intensities observed to the right and to the left of the incident beam direction, respectively, and  $\epsilon$  is called the left-right scattering asymmetry. It is well known that when particles with spin are scattered elastically from spin-0 nuclei, the polarization ( $P$ ) produced equals the asymmetry ( $A$ ) which would have been observed if the projectiles had been 100% polarized.<sup>15</sup> Thus one may write  $\epsilon = P_i A = P_i P$  and it follows that to determine  $P$  two experiments are needed, i.e., a measurement of the beam polarization  $P_i$  and a measurement of the left-right scattering asymmetry  $\epsilon$ .

The quantity  $\epsilon$  is sensitive to many false asymmetries, e.g., the asymmetries caused by misalignment of the incident beam in the scattering chamber, unequal angles for the two detectors, and differences in the geometries and efficiencies of the two detectors. These problems can be corrected to first order by placing a solenoid magnet upstream from the target which enables the direction of polarization of the beam to be rotated by  $\pi$  rad.<sup>1</sup> Such an arrangement allows the measurement of the following three independent asymmetries which may be combined to cancel effects due to spurious asymmetries:  $\epsilon_0$  = the asymmetry with no excitation of the solenoid,  $\epsilon_{cw}$  = the asymmetry with the solenoid rotating the spin direction clockwise,  $\epsilon_{ccw}$  = the asymmetry with the solenoid rotating the spin direction counterclockwise. The true asymmetry may be represented by the following expression:

$$\epsilon = \frac{1}{2} [\epsilon_0 + (\epsilon_{cw} + \epsilon_{ccw}) / 2 \cos \psi],$$

where  $\psi$  is the angle by which the solenoid rotates the direction of polarization ( $\psi \simeq 180^\circ$ ). The average of the asymmetries  $\epsilon_{cw}$  and  $\epsilon_{ccw}$  corrects for a possible shift in the centroid of the beam because of the solenoid. The average of this result with  $\epsilon_0$  cancels the remaining false asymmetries to a first-order approximation.

### B. Experimental Procedure

A highly polarized beam of protons was obtained by scattering the positive-ion beam of the cyclotron internally from a carbon scatterer (polarizer). The nominal radial and azimuthal settings of the polarizer were chosen such that the first pair of quadrupole

<sup>13</sup> J. M. Cameron, J. R. Richardson, W. T. H. van Oers, and J. W. Verba, preceding paper, Phys. Rev. **167**, 908 (1968).

<sup>14</sup> R. F. Carlson, W. F. McGill, J. M. Cameron, J. W. Verba, and J. R. Richardson, Bull. Am. Phys. Soc. **12**, 483 (1967).

<sup>15</sup> T. Y. Wu and T. Ohmura, *Quantum Theory of Scattering* (Prentice-Hall, Inc., Englewood Cliffs, N. J., 1962), p. 152.

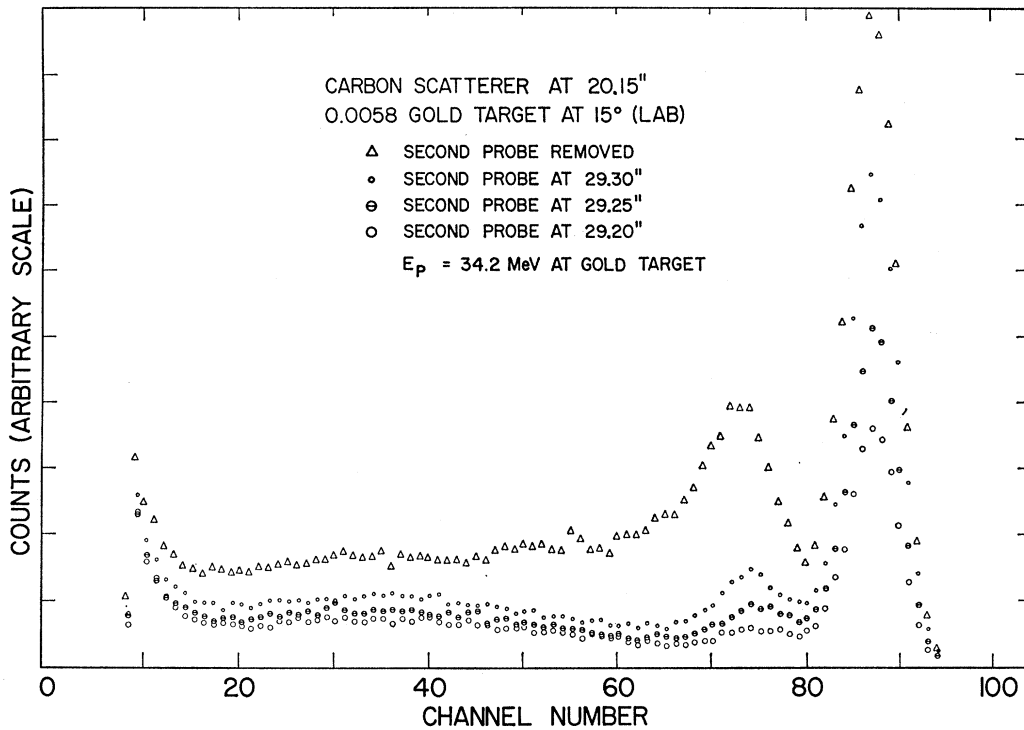


FIG. 1. Energy spectra of the polarized beam scattered from a gold foil for various positions of the second probe. The mean energy at the gold target was 34.2 MeV.

magnets, placed adjacent to the yoke of the cyclotron magnet, captured protons scattered at about  $55^\circ$  from the carbon vane in a cone with a half-angle of  $1.5^\circ$ . The energy of the polarized proton beam is initially determined by the thickness of the polarizer. The energy spread, however, imposed a lower limit on the energy which could be attained in this manner. For energies smaller than 34 MeV, aluminum degraders were inserted into the beam 4 in. before the target. The thicknesses of the carbon scatterers and aluminum degraders together with the corresponding energy spreads of the incident proton beams are given in Table I. The thickness of the degrader required was calculated using the range-energy tables of Barkas and Berger.<sup>16</sup>

The use of a carbon scatterer caused the polarized proton beam to be appreciably contaminated with lower-energy protons, e.g., a pronounced group of protons leaving  $C^{12}$  in the first excited state. A second probe was therefore inserted into the vacuum tank between the carbon vane and the exit port. Utilizing the fringing field of the cyclotron magnet, the intensity of inelastically scattered protons transported through the system of external beam optics could be greatly reduced (Fig. 1). The spectra of Fig. 1 were obtained by scattering the polarized proton beam from a gold foil at a laboratory angle of  $15^\circ$  (lab). It is seen that a

position of the second probe could be found which resulted in a large reduction in the low-energy contamination without a great sacrifice in intensity of the primary beam. The intensity of the polarized beam depended, of course, on the internal beam current and the thickness of the polarizer. With  $10 \mu A$  of internal beam on a 0.075-in.-thick carbon scatterer the external polarized beam had an intensity of  $\approx 5 \times 10^7$  protons  $\text{sec}^{-1}$ .

The general layout of the experiment is shown in Fig. 2. The first pair of quadrupole magnets produced a parallel beam of protons, which was passed through a 128-in.-long solenoid magnet. Finally, the beam was focused on the target at the center of a 10-ft-diam scattering stand by a second pair of quadrupole magnets. The beam was collimated by a 0.25-in.-wide by 0.50-in.-high slit placed 3.5 in. upstream from the target. At the collimator, the beam spot is about 0.5 in. wide by 1.0 in. high. Fourteen in. downstream from the target the dimensions of the beam are 0.5 in. by 1.0 in. At this position a split ionization chamber was mounted which continuously monitored the spatial position of the beam. A sufficient amount of aluminum absorber was placed in front of the ionization chamber to reduce the proton flux through it by one-half. By displaying the current from the polarizer and the difference and sum currents from the split ionization chamber, one may detect a shift in the centering of the beam as well as a change in the beam energy. To adjust for small changes in the energy, the amount of aluminum

<sup>16</sup> W. H. Barkas and M. J. Berger, *Tables of Energy Losses and Ranges of Heavy Charged Particles* (National Aeronautics and Space Administration, Washington, D. C., 1964).

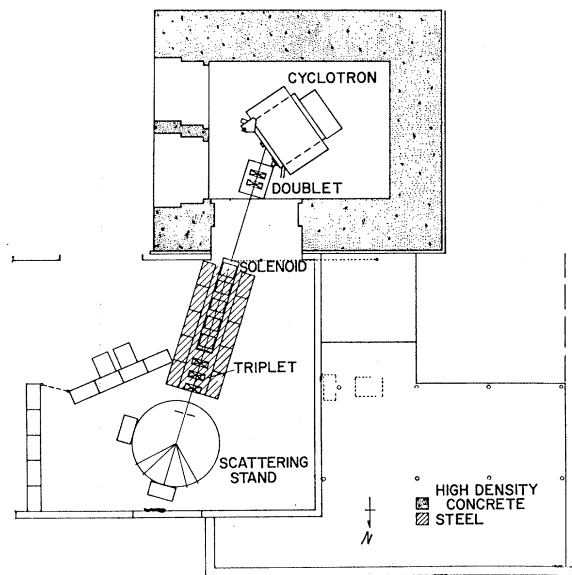


Fig. 2. Arrangement of beam optics for the polarized beam.

degrader in front of the target could be varied remotely. With a properly tuned beam and no drastic change in the cyclotron itself, a typical shift in the spatial position of the centroid of the beam spot at the target was  $(0.01 \pm 0.005)$  in. when the current in the solenoid was reversed. The energy of the beam was determined by measuring the range of the protons in calibrated aluminum absorbers placed in front of the split ionization chamber and using known range-energy relations.<sup>16</sup>

The target used was a disc of ice 0.032 in. thick by 1.25 in. diam, held in a copper frame by 0.00025-in.-thick Mylar foils. The copper frame was attached via a manifold to a reservoir filled with liquid nitrogen. Both target and manifold were encased within a 7-in.-diam evacuated scattering chamber. The entrance port to this chamber was covered with a 0.002 in. Mylar foil. The disc of ice was positioned at the center of the scattering chamber and could be rotated about a vertical axis through its center. Particles scattered from the target could exit from the chamber through a 2-in.-high slot covered with a 0.002-in.-thick Mylar foil and could be detected over the angular range from  $-165^\circ$  through  $+165^\circ$ .

Scattered particles were detected by four 2-in.-diam by 0.5-in.-thick NaI(Tl) integral line detectors which have a resolution of about 1.5% for 50-MeV protons. The detectors were placed in pairs at equal angles to the left and to the right of the incident beam. The detector assemblies had defining collimators 0.835 in. wide by 1.25 in. high immediately in front of the scintillation crystals. Snouts with antiscattering collimators prevented the scintillation crystals from being illuminated directly by the entrance foil and collimator of the chamber. All collimators were made from copper. Each of the two arms of the scattering stand carried

TABLE II. The counting geometry used in the  $p+O^{16}$  polarization measurements. The defining collimators were 0.835 in. wide by 1.25 in. high.

Angular region	Angular increments	Distance from the defining collimator to the target center	Target orientation	Angle between the two left or right counters
$15^\circ-72.5^\circ$	$2.5^\circ$	19.14 in.	normal to the beam	$15^\circ$
$65^\circ-120^\circ$	$5.0^\circ$	9.57 in.	rotated over $40^\circ$	$30^\circ$
$105^\circ-160^\circ$	$5.0^\circ$	9.57 in.	normal to the beam	$30^\circ$

two detector assemblies. The distance from the target center at which the detectors were mounted varied with the scattering angle. At the lower angles where the cross section is relatively large the detectors could be mounted at a greater distance from the target to give better angular definition, while at larger angles the angular resolution was sacrificed to give a reasonable counting rate. Pertinent information regarding the counting geometry used is indicated in Table II. The last column refers to the angle between the counters on the same arm of the scattering stand. Each of the two arms of the scattering stand could be rotated independently. The scattering angles could be read with an accuracy of  $\pm 0.1^\circ$ .

Pulses from each preamplifier were fed into a double-delay line amplifier. In the earlier stage of the experiment the pulses from the four linear amplifiers were fed into a four-channel mixer unit which routed the pulses from the four counters into separate 100 channel subgroups of the memory of an RIDL 400-channel pulse-height analyzer. A group of four typical spectra as displayed by the analyzer is shown in Fig. 3. Later, the pulses from the four linear amplifiers were gated and analyzed by the SDS 925 computer operating in a fourfold single-parameter mode. Each of the spectra was recorded in 128 channels.

### C. Data Reduction

The spectra from the various detectors recorded by the pulse-height analyzer were punched on cards, while the spectra recorded by the SDS 925 computer were stored on magnetic tape to facilitate further analysis.

Since the target contained hydrogen and oxygen, the peaks in the spectra corresponding to protons elastically scattered from these elements partially overlapped at forward angles. At larger angles, peaks corresponding to the elastic group of protons in the beam inelastically scattered from the target and the inelastic group of protons in the beam elastically scattered from the target superimposed on a continuous background became more and more important. These facts, combined with the energy resolutions present, required the experimental spectra to be unfolded in two or more peaks of Gaussian

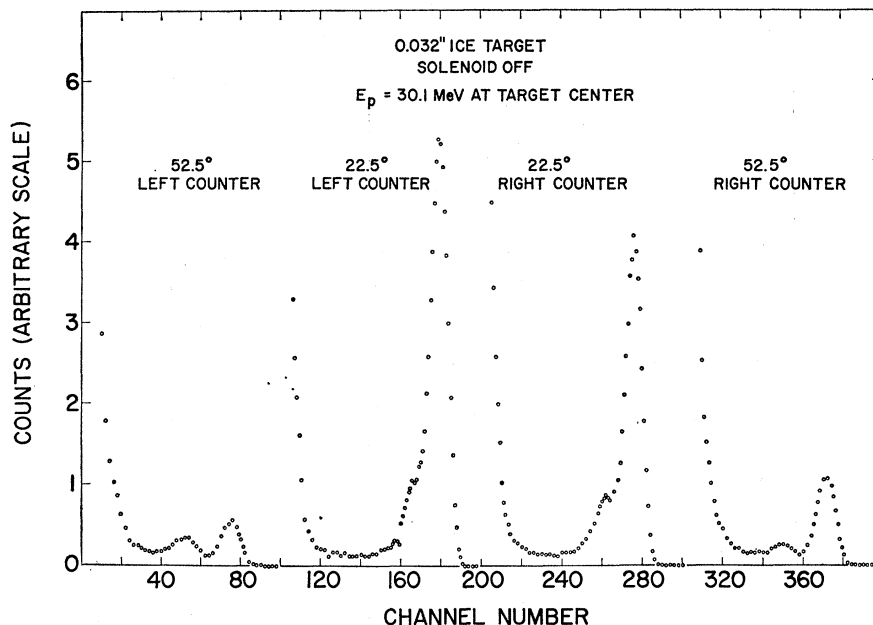


FIG. 3. Typical spectra for the scattering of the polarized beam from the ice target as displayed by the 400-channel pulse-height analyzer.

form and some functional background in order to obtain the number of counts corresponding to protons elastically scattered from oxygen. The spectrum stripping routine was based upon minimizing  $\chi^2$  where

$$\chi^2 = \sum_{i=1}^n \frac{[N_i(\text{theor}) - N_i(\text{expt})]^2}{N_i(\text{expt})}$$

The number of counts in the  $i$ th channel is denoted by  $N_i(\text{expt})$ . The calculated number  $N_i(\text{theor})$  is the sum of the contributions for the  $i$ th channel due to the elastic peak or peaks, any inelastic components and an appropriate background or continuum. The first step in the analysis was to plot the recorded spectra. Visual inspection of these graphs gave an initial set of approx-

imate values for the parameters of the Gaussians. Also it could be determined whether the background could be represented by a linear, a cubic, or an exponential function. The next step was the actual peak fitting in which an automatic search code varied the parameters from these initial values, producing the area under the Gaussian corresponding to the elastic group of protons in the beam elastically scattered from oxygen. To obtain consistent results all the spectra were analyzed in the above described manner. The spectrum stripping was performed using the IBM 7094 computer of the UCLA computing network and later the Philco 2000 system at the University of Wyoming.<sup>17</sup>

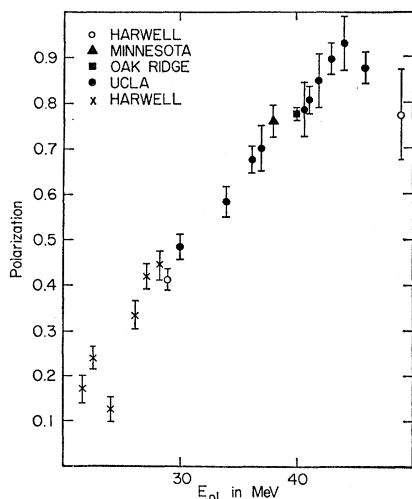


FIG. 4. The polarization in  $p-C^{12}$  elastic scattering at a laboratory scattering angle of  $55^\circ$  as function of incident energy. Harwell,  $\circ$  Ref. 2; Minnesota,  $\blacktriangle$  (Ref. 4); Oak Ridge,  $\blacksquare$  Refs. 5 and 6; UCLA,  $\bullet$ ; Harwell,  $\times$  Ref. 8.

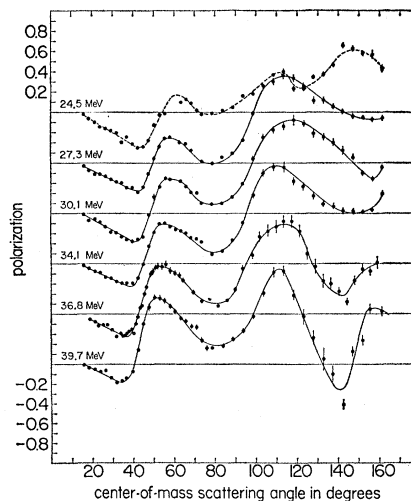


FIG. 5. Polarization angular distributions for  $p-O^{16}$  elastic scattering at mean proton energies of 24.5, 27.3, 30.1, 34.1, 36.8, and 39.7 MeV.

<sup>17</sup> We wish to acknowledge the helpful cooperation of the Computing Center at the University of Wyoming.

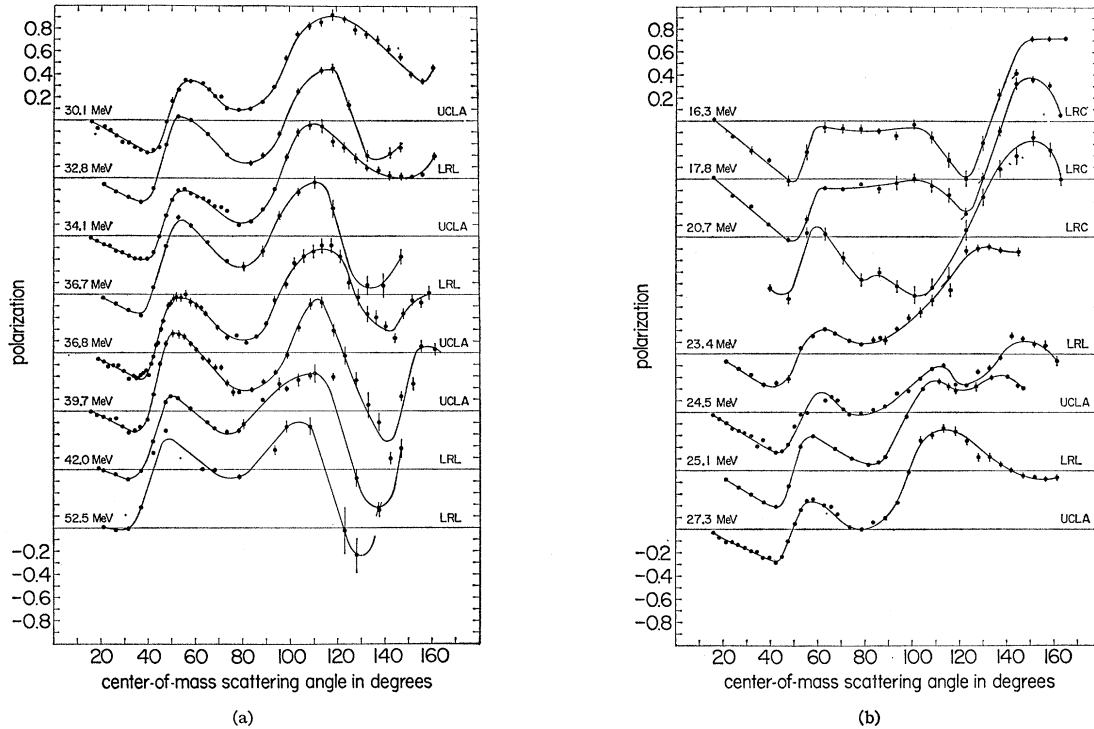


FIG. 6. (a) Comparison between the present polarization angular distributions at 30.1, 34.1, 36.8, and 39.7 MeV with the data of Boschitz *et al.* (Ref. 11) at 32.8, 36.7, 42.0, and 52.5 MeV. (b) Comparison between the present polarization angular distributions at 24.5 and 27.3 MeV with the data of Boschitz *et al.* (Ref. 11) at 16.3, 17.8, 20.7, 23.4, and 25.1 MeV.

The areas under the Gaussians of interest were introduced in the formula for the left-right asymmetry  $\epsilon$ . The areas are indicated according to the usual notation as  $L$  and  $R$ . Then, following the Basel convention,

$$\epsilon(\theta) = \left[ \frac{1}{2} \frac{R_0 - L_0}{R_0 + L_0} + \frac{1}{2 \cos \psi} \frac{R_{cw} - L_{cw}}{R_{cw} + L_{cw}} + \frac{1}{2 \cos \psi} \frac{R_{ccw} - L_{ccw}}{R_{ccw} + L_{ccw}} \right],$$

where the subscripts 0, cw, and ccw refer to the various rotations of the spin direction in the solenoid magnet as defined above, and  $\psi$  is the angle of rotation ( $\psi \approx 180^\circ$ ). The errors in the asymmetry  $\epsilon(\theta)$  were computed from the errors in the independent quantities  $R_0$ ,  $L_0$ ,  $R_{cw}$ ,  $L_{cw}$ ,  $R_{ccw}$ ,  $L_{ccw}$ , and  $\psi$ . Only the statistical errors in the number of counts were included. No attempt was made to determine the error introduced by the spectrum-stripping procedure.

#### D. Measurement of the Beam Polarization

A calibration of the beam polarization is required to determine from the measured asymmetries the polarizations which will be present if an unpolarized beam of the same energy is scattered from the target. Since the polarized beam was produced by an initial scattering from a carbon vane (0.020, 0.075, 0.109, 0.140, and 0.180 in. thick) the mean energy of the first scattering differs appreciably from that of the second scattering,

and an indirect method for the measurement of the polarization is needed.

The technique used was based upon a determination of the ratios of the polarizations resulting from the various scatterers ( $P_1 - P_5$ ) to the polarization resulting from the 0.109-in.-thick scatterer ( $P_3$ ) as a function of energy. The various ratios were deduced from left-right asymmetries observed in scattering the polarized beam from carbon at a laboratory scattering angle of  $55^\circ$ . Below 43 MeV, i.e., for the 0.109-, 0.140-, and 0.180-in.-thick vanes, the ratio appeared to be quite linear. Consequently, we could extrapolate to an energy corresponding to the energy of second scattering of a measured asymmetry. The extrapolated ratio was combined with that asymmetry and a measured ratio to solve for one of the beam polarizations in a set of three equations with three unknowns. The value obtained could be used to solve for the remaining unknown polarizations. The results are shown in Fig. 4. There are two main consistency checks which can be applied to this calculation. First, the curve of polarization versus energy should be reasonably smooth above 30 MeV. It was found that a discontinuity appeared between 37 and 40 MeV if the curve was improperly normalized. Second, there should be good agreement with the existing experimental data which can be considered to be fairly accurate. Inspection of Fig. 4 shows that there is good agreement with the data point

at 40 MeV.<sup>5,6</sup> The present data also join smoothly with the data from the Rutherford High Energy Laboratory between 20 and 28 MeV.<sup>8</sup> There is also reasonable agreement with the data points at 29 and 49 MeV.<sup>2</sup> The data point at 38 MeV,<sup>4</sup> however, appears somewhat high. The polarization at 55° lab appears to be a rather smooth function of energy except in the lower-energy region, i.e., below 26 MeV. The values for the beam polarizations are included in Table I.

### III. RESULTS AND DISCUSSION

The polarizations in the elastic scattering of protons from oxygen at 24.5, 27.3, 30.1, 34.1, 36.8, and 39.7 MeV are shown in Fig. 5. The polarization  $P(\theta)$  was ascertained from the left-right asymmetry  $\epsilon(\theta)$  and the incident beam polarizations  $P_i$ , using

$$P(\theta) = \epsilon(\theta)/P_i.$$

The polarization angular distributions show a monotonic energy variation between 30 and 40 MeV. The data at 24.5 and 27.3 MeV, however, indicate a departure from such a smooth energy variation.

A comparison with the available data<sup>11</sup> in the energy region under consideration shows agreement with the observed trends. In Fig. 6(a) we compare our measurements at 30.1, 34.1, 36.8, and 39.7 MeV with the data from Boschitz *et al.*<sup>11</sup> at 32.8, 36.7, 42.0, and 52.5 MeV. The agreement in the angular region of 15°–120° c.m. is good. The diffraction patterns change smoothly as the incident proton energy increases. For the angular region beyond 120° c.m. the agreement between the two sets of data is less spectacular, the last minimum in the present set of angular distributions being less pro-

nounced. No explanation for this discrepancy has been found. In Fig. 6(b) we compare our measurements at 24.5 and 27.3 MeV with the data from Boschitz *et al.*<sup>11</sup> at 16.3, 17.8, 20.7, 23.4, and 25.1 MeV. Drastic changes in the polarization pattern occur between 21 and 27 MeV. A similar irregular variation in the polarization angular distributions for the elastic scattering of protons by carbon was observed by Craig.<sup>8</sup> Subsequently, the elastic differential cross sections<sup>9</sup> and polarizations for the scattering of 20–28-MeV protons by C<sup>12</sup> were analyzed by Lowe and Watson<sup>10</sup> by the addition of scattering from three states in N<sup>13</sup> to the optical-model scattering. Recently, Scott *et al.*<sup>18</sup> discussed some of the anomalies in the elastic and inelastic scattering of nucleons by C<sup>12</sup> in the energy range from 20 to 30 MeV. They suggest that these effects are due to three simple compound states in N<sup>13</sup> at a high level of excitation. They show by means of direct reaction theory that these states are closely associated with single-particle resonances, and that they are likely doorway states of three-quasiparticles. The irregular nonmonotonic energy behavior that appears to be present in the elastic differential cross sections as shown in the preceding paper<sup>13</sup> and polarizations for the scattering of 20–30-MeV protons by O<sup>16</sup> might reflect the presence of similar states in F<sup>17</sup>. The general appearance of the polarization data above 30 MeV seems to be compatible with an optical-model description for the  $p$ -O<sup>16</sup> interaction. An optical-model analysis of the polarization data combined with differential cross section and total reaction cross section data is in progress.

<sup>18</sup> D. K. Scott, P. S. Fisher, and N. S. Chant, Nucl. Phys. **A99**, 177 (1967).